

SIMULATION OF MAIN ROTOR NOISE EMISSION GENERATED DUE TO BLADE THICKNESS

R. M. Mirgazov, V. A. Golovkin, B. S. Kritsky
Central Aerohydrodynamic Institute named after N. E. Zhukovsky (TsAGI)
Zhukovsky, Russia

The thickness noise generation by rotor is studied, i. e. the main rotor noise dependence on its blades thickness. In this case both the physical blade thickness and the nonlinear effect of the blade tip section near-sonic flow are of importance. In this paper the influence of blade physical thickness on the thickness noise only was studied. The model of main rotor noise emission due to blade thickness is based on the linear acoustic theory. It allows studying the noise mechanism and evaluating the influence of different blade parts on its level as well as giving the recommendations concerning the choice of tip section shapes and profile thicknesses with the view to alleviate the thickness noise. Some examples are given to estimate the noise pressure in different points in space for various rotor configurations and different operating modes.

1. INTRODUCTION

Since ICAO toughens the requirements concerning flight vehicle noise the study of acoustical influence of helicopter main rotor comes into importance. It is related to higher environment compatibility of advanced and modernized helicopters. Therefore the evaluation of rotor noise emission and specific measures of its reduction are reasonable on the feasibility conceptual stages.

Helicopters are complex flight vehicles in the context of aerodynamics and wide range of physical processes. The noise pattern is especially complicated [1,2]. Let us distinguish the noise due to the helicopter major component – its main rotor. It is complex as for its structure. We distinguish the vortex noise, the rotational noise and the blade slaps [2]. When M number at the advancing tip of main rotor increases up to 0.85 and more the generated sound emission is drastically directed forward in the nature of narrow peaks of negative pressure having the same frequency as blade rotations. This noise emission is subjectively perceived as rather disturbing shocks. Studies show [3,

4, 5] that this noise is generated by blade flow air displacement since the blade thickness is finite. Thus it matters the very physical thickness of blade as well as the nonlinear effect of blade tip section near sonic flow which is similar in action. Therefore the exact studies of near sonic impulse noise of main rotor require the evaluation of blade flow velocity field. This study investigates only the influence of blade physical thickness.

We used the generic linear acoustic equations which of solution was made with methods [4, 5] which establish a simple solution for the sound pressure field of arbitrarily moving line with travel-speed-oriented dipoles. On this basis we developed a practical method to calculate the sound pressure field of helicopter rotor blade [6] stipulated by its thickness. It was specified that the found solution was in satisfactory agreement with the sound pressure measurement data [1, 7]. The solution allows analyzing the influence of different blade sections on the sound pressure level and giving recommendations to choose the blade tip shape and profile thicknesses that will restrict the thickness noise.

Below we enunciate the developed method and results of computational studies which are to evaluate the influence of blade tip shape and blade tip velocity on the sound pressure peaks stipulated by blade thickness effect.

2. PROBLEM STATEMENT

The infinite quite gas is considered which is disturbed since the time $t=0$ due to appearance of sources distributed on some transparent for gas surface w (Figure 1) having the mass per area $Q(\vec{r}, t)$ depending on the radius – vector \vec{r} of the source position and on the time.

The wave equation is given by:

$$\Delta\varphi_n - \frac{1}{a^2} \frac{\partial^2 \varphi_n}{\partial t^2} = 0. \quad \text{For acoustic}$$

approximation the velocity \vec{v} and the pressure p of flow disturbed by sources are:

$$\vec{v} = \text{grad}\varphi_n, \quad p = -\rho \frac{\partial \varphi_n}{\partial t},$$

Where velocity potential φ_n is defined by the integral:

$$\varphi_n(\vec{r}_0, t_0) = -\frac{1}{4\pi} \iint_{w_*} \frac{1}{l} Q(r, t_0 - \frac{l}{a}) ds.$$

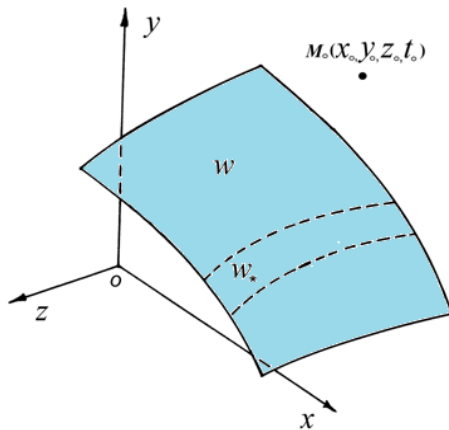


Figure 1 – Problem statement

Where a – sound velocity, ρ – undisturbed gas density, $l = |\vec{r} - \vec{r}_0|$ distance between the integration point \vec{r} on the surface w and the point of application \vec{r}_0 . The integration domain w_* consists of surface points where the function $Q(r, (t_0 - l/a))$ of retarded time $(t_0 - l/a)$ is different from zero. Let us accept that the domain where the source density $Q(\vec{r}, t)$ is different from zero represents the infinitely narrow strap $w_0(t)$ moving along the surface w .

3. METHOD AND ALGORITHM OF CALCULATION

Let the rotor hub moves at the constant speed V and comes to the moment t in the reference point of coordinate axis $oxyz$ (Figure 2). The linear acoustic theory provides the following expression for the acoustic pressure generated by blade thickness $h(x, \vec{r})$ at the moment t in the point $M_p(x_p, y_p, z_p)$ of main rotor far field:

$$p(\vec{r}) = -\frac{\rho a^2 M_k^2}{4\pi(l_*/R)} \left(\frac{a}{a_{np}}\right)^3 \int_0^1 d\bar{r} * \int_{x_1}^{x_2} h(x, \vec{r}) \delta(\bar{\psi} + \frac{x}{r}) dx \quad (1)$$

Here $\vec{r} = r/R$ is a relative radius of section and x – coordinate along the chord defined for the direction from leading edge to trailing edge. The parameter $\bar{\psi}$ plays the role of non-dimensional time and is related to simple azimuthal angle of blade $\psi = \omega t$ by the relation:

$$\psi = \bar{\psi} + \frac{\omega}{a} l_* + \varphi + \frac{3}{2} \pi. \quad (2)$$

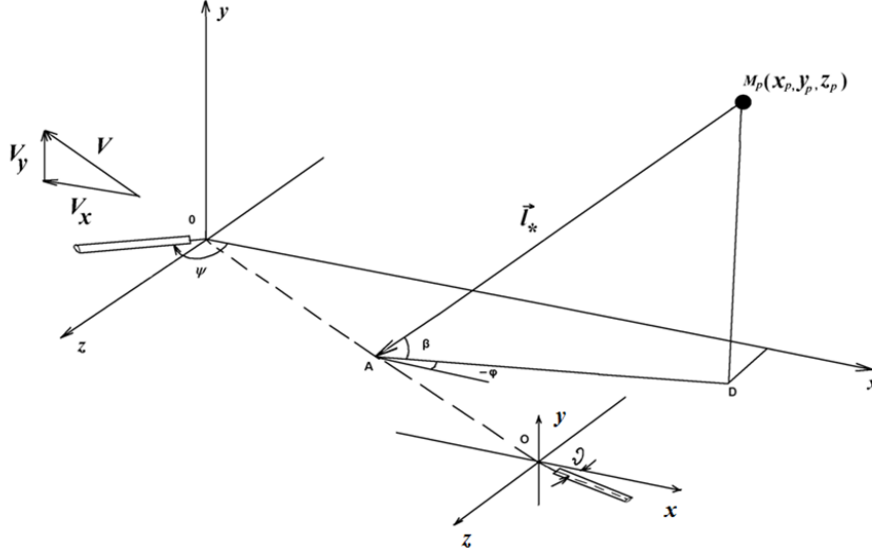


Figure 2 – Computational scheme

By means of l_* in (1) and (2) the distance between the point $M_p(x_p, y_p, z_p)$ and the centre of main rotor hub at a design point of time is specified:

$$l_* = (-B + \sqrt{B^2 + AC}) / A.$$

Here

$$\begin{aligned} A &= 1 - M_x^2 - M_y^2, \\ B &= x_p M_x - y_p M_y, \\ C &= x_p^2 + y_p^2 + z_p^2, \end{aligned}$$

while $M_x = V_x / a$, $M_y = V_y / a$ – are relations of tangential V_x and normal V_y rotor disk helicopter velocity component to the sound velocity a . Besides the sound velocity a in the formula (1) there is also a parameter a_{np} defined as follows:

$$a_{np} = a + V_x \cos \beta \cos \varphi - V_y \sin \beta,$$

Where angles β and φ are defined by the relations

$$\begin{aligned} \sin \beta &= \frac{(y_p + l_* M_y)}{l_*}, \quad \cos \beta = \sqrt{1 - \sin^2 \beta}, \\ \sin \varphi &= \frac{z_p}{l_* \cos \beta}, \quad \cos \varphi = \frac{(x_p - l_* M_x)}{l_* \cos \beta}. \end{aligned}$$

The function $\delta(\bar{\psi} + \frac{x}{r})$ in (1) is defined through the parameter \mathcal{G}

$$\delta(\mathcal{G}) = \frac{1}{(1 - u \cos \mathcal{G})^4} \left[u \cos \mathcal{G} - \frac{3u^2 \sin^2 \mathcal{G}}{1 - u \cos \mathcal{G}} \right]$$

\mathcal{G} , $\bar{\psi}$ and x are related by the equation:

$$(3) \quad \mathcal{G} - u \sin \mathcal{G} = \bar{\psi}_\Sigma,$$

where $\bar{\psi}_\Sigma = \bar{\psi} + x / r$.

Here the value u is defined: $u = u_k \bar{r}$,

where $u_k = \frac{\omega R \cos \beta}{a_{np}}$. The tip M number in

(1) is equal to $M_k = \omega R / a$. The value $h(x, \bar{r})$ in (1) specifies the distance between the upper and lower surfaces of blade measured as a normal to the surface of rotor disc.

The variable of integration \mathcal{G} for internal integral (1) results in:

$$(4) \quad p(\bar{\psi}) = -\frac{\rho a^2 M_k^2}{4\pi(l_*/R)} \left(\frac{a}{a_{np}}\right)^3 \int_0^1 \bar{r} d\bar{r} * \int_{\mathcal{G}_1}^{\mathcal{G}_2} \frac{h(x, \bar{r})}{R} \frac{u \cos \mathcal{G} (1 + 2u \cos \mathcal{G}) - 3u^2}{(1 - u \cos \mathcal{G})^4} d\mathcal{G}$$

Limits of integration \mathcal{G}_1 and \mathcal{G}_2 in (4) are defined by the equations:

$$(5) \quad \begin{aligned} \mathcal{G}_1 - u \sin \mathcal{G}_1 &= \bar{\psi} + x_1 / r, \\ \mathcal{G}_2 - u \sin \mathcal{G}_2 &= \bar{\psi} + x_2 / r, \end{aligned}$$

The variable x in $h(x, \bar{r})$ is defined depending on the angle ϑ by the equation:

$$(6) \quad x = r(\vartheta - u \sin \vartheta - \bar{\psi}).$$

The explicit dependence (5) of variable x on ϑ allows avoiding the necessity to solve the equation (3) at each integration step (1) that sufficiently accelerates the calculations. The conversion of sound pressure into noise for PNL system is made according to

formula: $PNL = 20 \log \frac{p_m}{p_0}$ [dB], where $p_0 = 0.00002$ [Pa].

For the numerical implementation the blade thickness $h(x, \bar{r})$ was specified with two-dimensional tables for the range of radius values and the coordinate x (Figure 3).

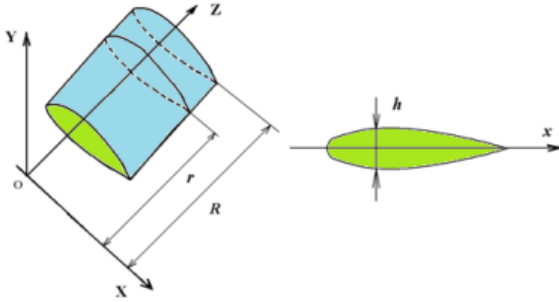


Figure 3 – Numerical implementation of blade thickness

The value h at a current point x, \bar{r} was specified by means of linear interpolation. Integrals were taken for proportional partition of x and \bar{r} using the rectangular formula. It is worth noting that the equation (6) has the sole solution for ϑ only if $u < 1$, that complies with subsonic normal speed

of blade sections. If $u > 1$ these formulas are not suitable.

4. CALCULATION RESULTS, COMPARISON WITH TEST

To approve the calculation method the flight test data were investigated and compared with the calculations data. The calculations defined the sound pressure in the direction of maximum sound radiation generated by the blade thickness pressure at vertical and horizontal planes that was defined experimentally [1, 7] (Figure 4 and 5). As the graphs show the sound pressure peak is reached at the advancing blade if the angle of radiation at vertical and horizontal planes is near to zero ($\alpha \sim 0, \beta \sim 0$). The distance between the main rotor hub and the microphone was $\ell = 3R \approx 29$ m, the relative flight velocity of helicopter is $\bar{V} = V/\omega R = 0,265$. It is seen that the number of sound pressure surges per one revolution is two, i. e. it is multiply to the number of the main rotor blades in the test (along the abscissa – non-dimensional time). The flight experiment procedure is shown in Figure 6. Figure 7 shows the comparison of calculation results obtained by the developed method and those obtained by the flight test.

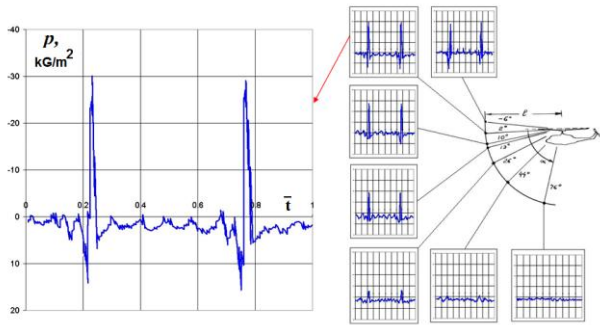


Figure 4 – Sound pressure levels at vertical plane

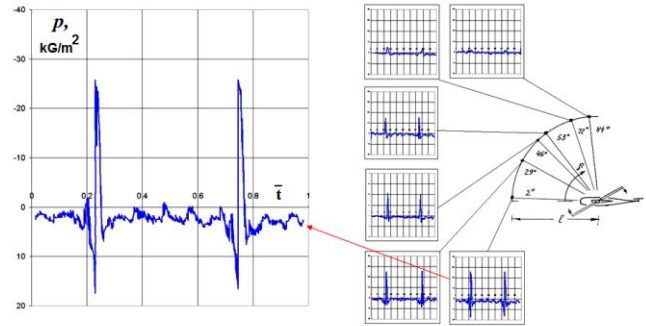


Figure 5 – Sound pressure levels at horizontal plane

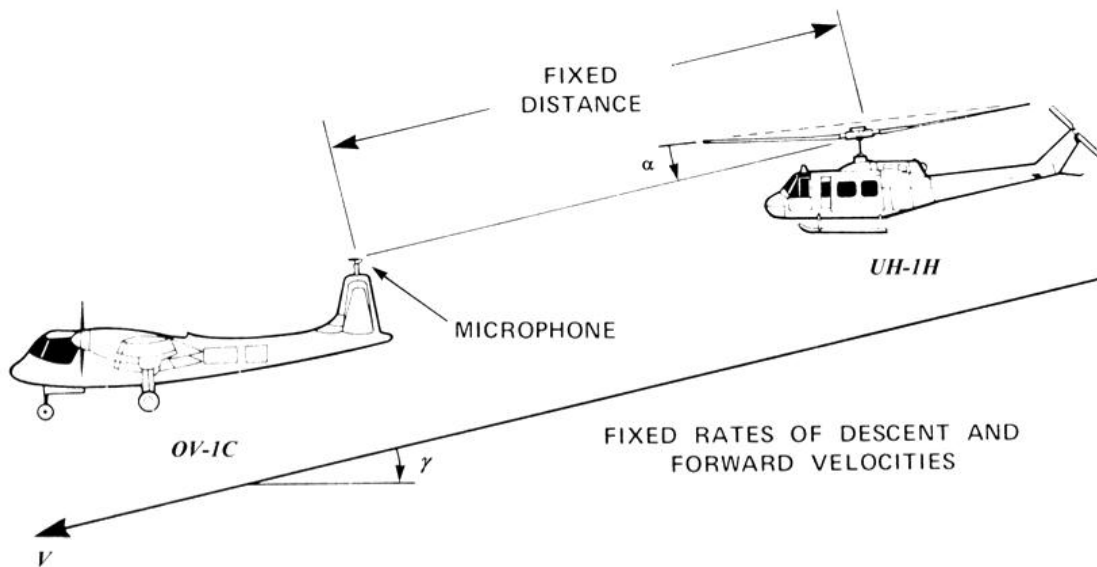


Figure 6. – Flight experiment procedure

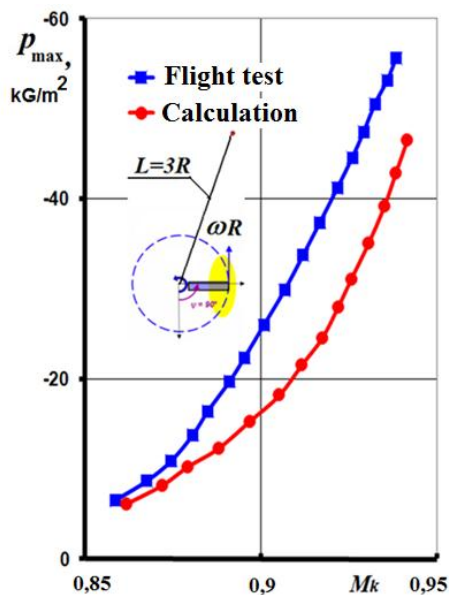


Figure 7 – Comparison of calculation results and flight test data

Both the calculations and the tests the curves represent the sound pressure peak values. Here $M_k = (\omega R + Vx)/a$ is total M number of advancing blade tip. The flight parameters and the main rotor blade characteristics were the following: the rotor radius is $R = 7.315 \text{ m}$, the blade chord is $b = 0.533 \text{ m}$, the blade profile is *NACA 0012* (characteristics of UH-1H helicopter), the rotor tip velocity is $\omega R = 248 \text{ m/s}$, the flight velocity changed in the range of $Vx = 45 \dots 70 \text{ m/s}$. The curve of test data shows the total contribution of all helicopter noise components and the curve of proposed calculations method shows the value of sound pressure dynamic peak stipulated only by the blade thickness

effect. Due to the graph it follows that the sound pressure peak values estimated by this method are stipulated by the blade thickness effect and make 70...75% of test values at an advancing blade.

According to the developed method the parametric analysis was made to evaluate qualitatively the influence of different blade geometric parameters, particularly its tip, and the flight parameters influence on the maximum peak of sound pressure. There are many various blade tips. Some of them are shown on Figure 8.

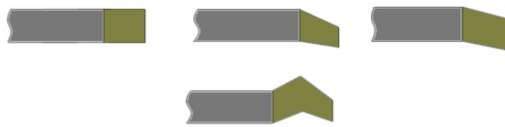


Figure 8 – Generic tips of main rotor blade

The calculations were performed for different rotor blade geometric shapes: rectangular, swept, (χ), tapered (η), and swept-tapered types with radius $R=8$ m, chord $b=0.4$ m and relative thickness $\bar{c} = 6 \%, 9 \%, 12 \%, 15 \%$. The point of pressure estimation was on the rotor-fixed axis located before the rotor at the distance of 3 rotor radiuses from the hub ($\alpha \sim 0, \beta \sim 0$). It was assumed that the azimuth is calculated from the position of advancing blade, thus angles $\bar{\psi}$ and ψ agree. Rotor velocity is $V_x = 80$ m/s, tip speed is $\omega R = 250$ m/s.

Figure 9 shows the characteristic dependence for the sound pressure of rectangular blade in the domain of its maximum at $V_x = 80$ m/s, $\omega R = 250$ m/s, $\bar{c} = 12 \%$. Thus the comparison of further calculation results is more comfortable. This is due to the fact that the profile relative thickness $\bar{c} = 12 \%$ (NACA 0012) is the most widespread and well-studied in calculation aerodynamics models of as well as in tests.

It allows evaluating the sound pressure generated by physical thickness for a blade profile NACA 23012, which was used at helicopters Mi - 8 and others.

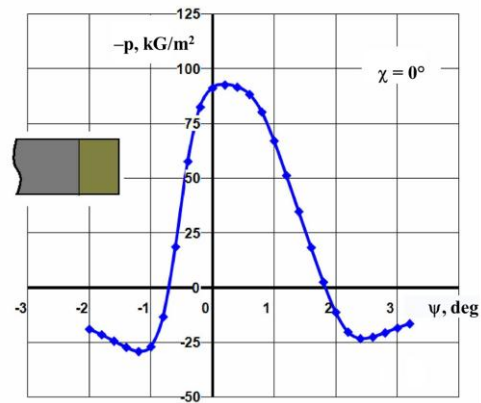


Figure 9 – Dependence of sound pressure for rectangular blade

Figure 10 shows the pressure distribution $-p$ [kgs/m²] at $\bar{c} = 15 \%$ and various tip sweep angles in peak region.

As Figure 10 shows the width of negative sound pressure peak is about $\Delta\bar{\psi} = 3^\circ$ that corresponds merely to $\Delta t \sim 1/500$. Such a pressure is subjectively perceived like a sharp loud shocks. The intensity of shocks is characterized by the value of peak region which makes in this case about -111.38 kgs/m². It is seen that the sound pressure peak height is sufficiently reduced if a small section of rectangular blade tip has a sweep angle (about 40°).

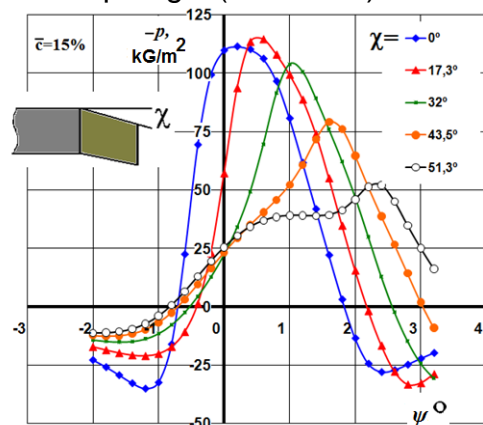


Figure 10 – Distribution of sound pressure in the region of its maximum for swept blade tip at relative thickness $\bar{c} = 15 \%$

The similar effect is seen on the following Figures (Figures 11, 12, 13) at different relative thickness $\bar{c} = 12\%$, 9% and 6% . The maximum sound pressure and its shift change while levelling the peaks in dependence on the specified blade tip shape and its relative thickness.

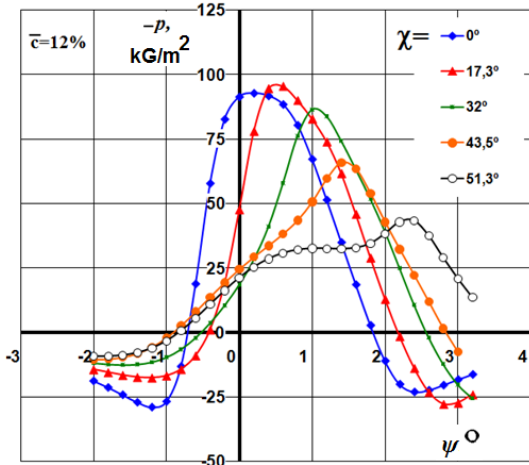


Figure 11 – Distribution of sound pressure in the region of its maximum for swept blade tip at relative thickness $\bar{c} = 12\%$

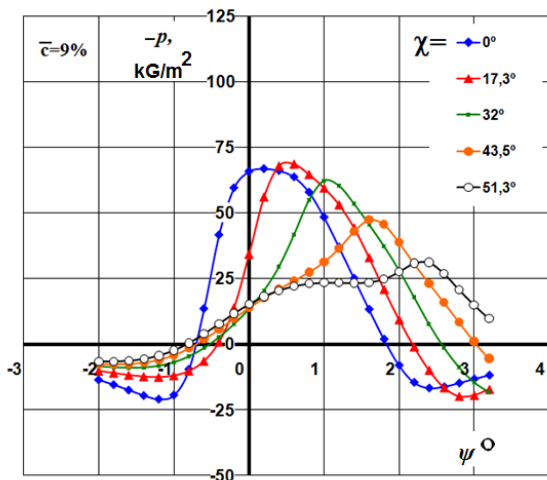


Figure 12 – Distribution of sound pressure in the region of its maximum for swept blade tip at relative thickness $\bar{c} = 9\%$

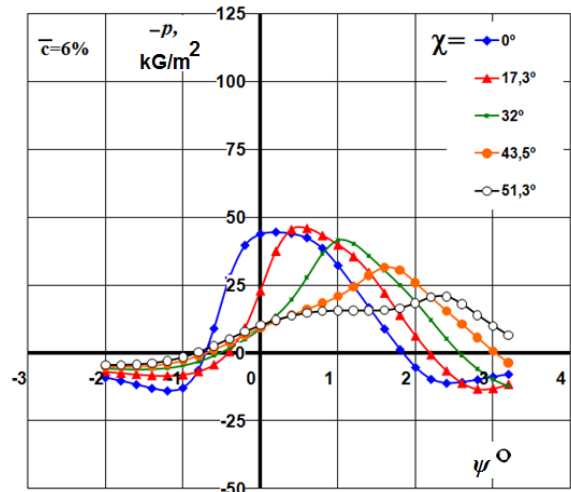


Figure 13 – Distribution of sound pressure in the region of its maximum for swept blade tip at relative thickness $\bar{c} = 6\%$

Figure 14 shows the evaluation of maximum sound pressure for tapered tips. It is seen that the taper η also influences on the p_{max} , and reduces its absolute value.

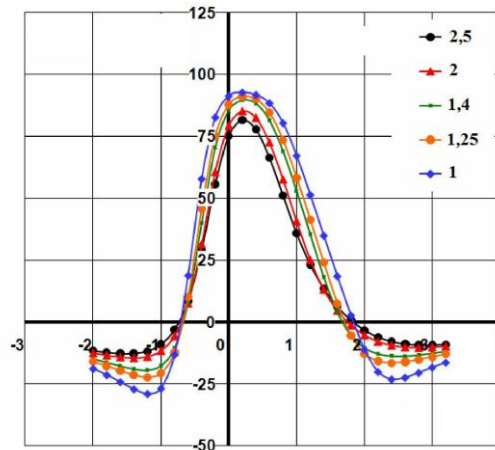
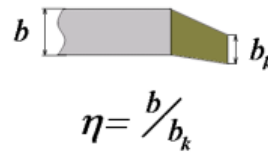


Figure 14 – Distribution of sound pressure for different tapers of blade tip at relative thickness $\bar{c} = 12\%$

Figures 15, 16, 17 and 18 show the results of sound pressure calculations for swept-tapered blade tips at different initial relative

thickness of blade tip. As it is seen such a type of blade tip significantly reduces the sound pressure.

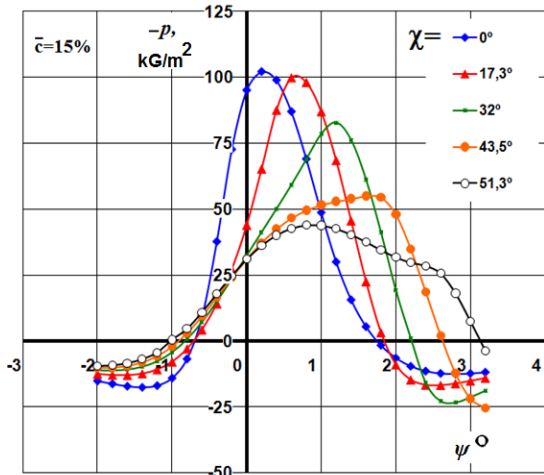
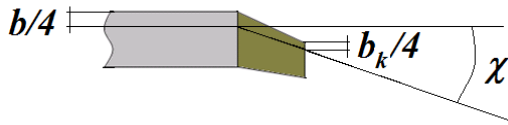


Figure 15 – Distribution of sound pressure in the region of its maximum for swept-tapered blade tip at relative thickness $\bar{c} = 15\%$

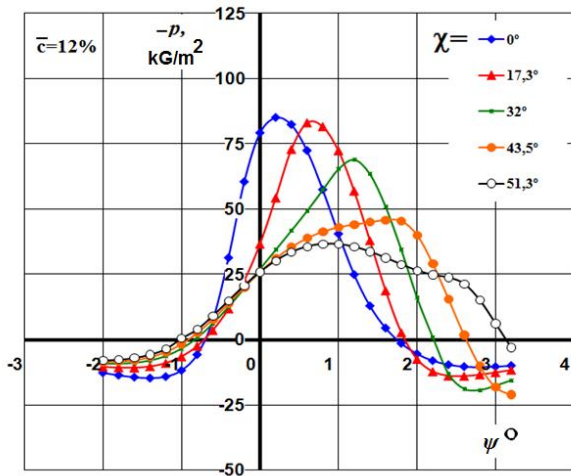


Figure 16 – Distribution of sound pressure in the region of its maximum for swept-tapered blade tip at relative thickness $\bar{c} = 12\%$

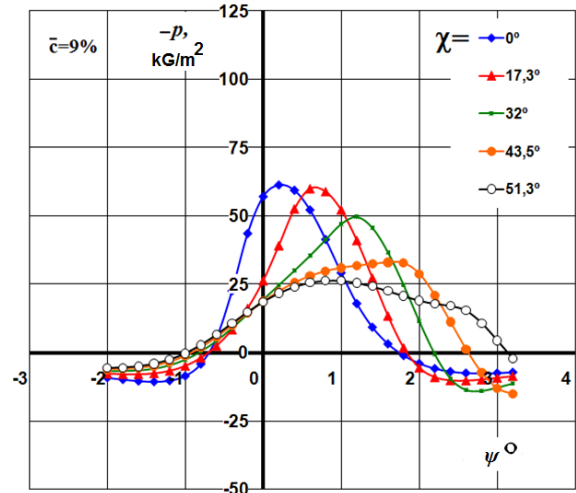


Figure 17 – Distribution of sound pressure in the region of its maximum for swept-tapered blade tip at relative thickness $\bar{c} = 9\%$

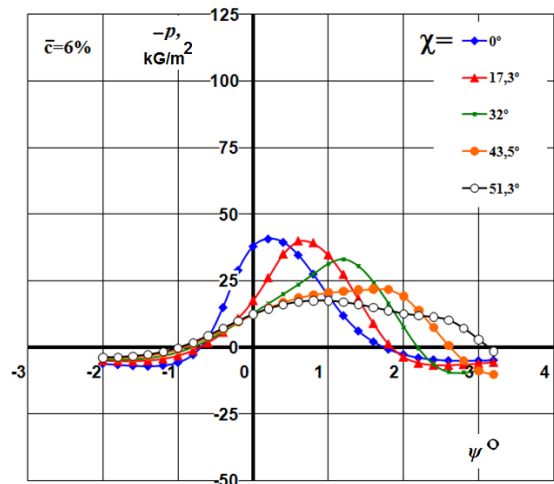


Figure 18 – Distribution of sound pressure in the region of its maximum for swept-tapered blade tip at relative thickness $\bar{c} = 6\%$

As Figure 19 shows if tip M numbers are high ($M \approx 0.9$ and more) the blade physical thickness is of great influence. If the relative thickness is increased from 6 % to 15 % (rectangular blade) the maximum sound pressure increases more than twice.

The similar result takes place for tapered tips (Figure 20).

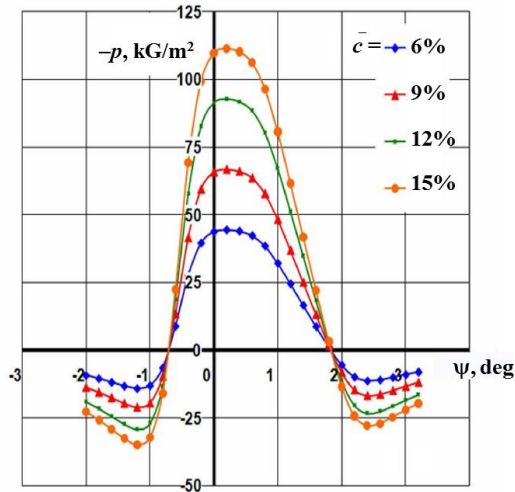


Figure 19 – Distribution of sound pressure for rectangular tips at different relative thickness and taper $\eta=1$, $\chi=0$

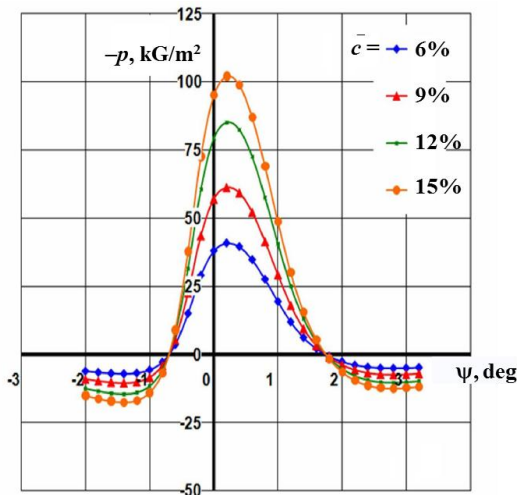


Figure 20 – Distribution of sound pressure for rectangular tips at different relative thickness and taper $\eta=2$, $\chi=0$

Figures 21 and 22 show dependences of the maximum sound pressure as a function of blade relative thickness.

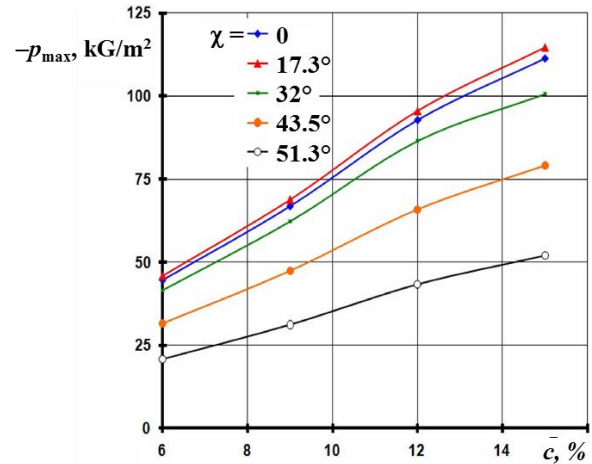


Figure 21 – Dependence $-p_{max}$ of sound pressure and blade tip relative thickness, taper $\eta=1$

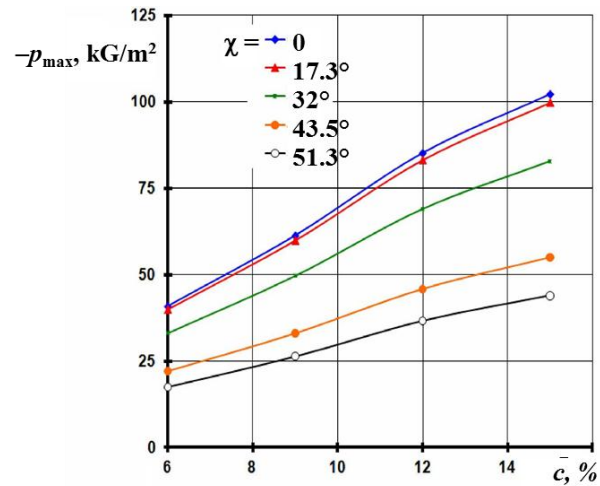


Figure 22 – Dependence $-p_{max}$ of sound pressure and blade tip relative thickness, taper $\eta=2$

It is seen that the sound pressure increases if the relative thickness augments at any sweep angle. At constant $-p_{max}$ we can choose any blade tip which has different relative thickness, sweep, taper that may satisfy other rotor characteristics, particularly the aerodynamic ones i. e. an optimum full solution for these or those tasks considered while determining the flight vehicle performance characteristics.

Figure 23 shows the influence of rectangular and tapered blades tip speed ωR on the sound pressure peak height $-p_{max}$. When the tip speed ωR increases

from 235 m/s to 250 m/s the value $-p_{max}$ augments more than fivefold.

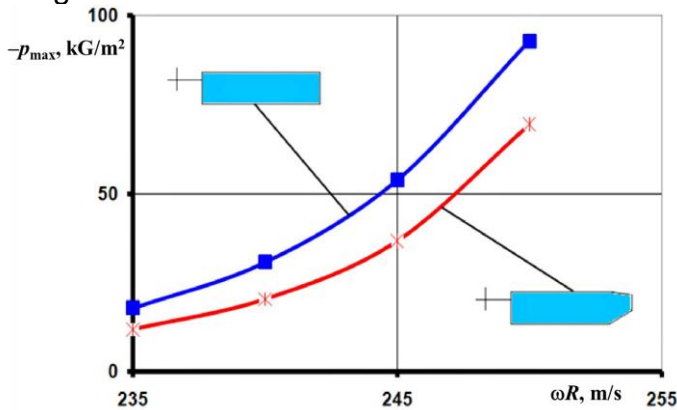


Figure 23 – Influence of rectangular and tapered blade tip speed on the value of maximum sound pressure

The development of the main rotor blade configuration allows choosing the rational geometric parameters (relative thicknesses, sweep angle, tip taper) that satisfy various conflicting requirements. These are the studies that have shown (Figures 24, 25) that the specified level of sound pressure can be provided with the appropriate values of blade tip relative thickness and its sweep angle χ .

It is defined that for non-tapered swept tips (Figure 24) the computational dependence $\chi(\bar{c})$ can be approximated by the power function $\chi(\bar{c}) = 36(\bar{c} - \bar{c}_0)^{0.18}$. Here \bar{c}_0 is a relative thickness at the sweep angle $\chi=0$. The study has established a similar equation for tapered swept blade tips (Figure 25). It can be approximated by the power function $\chi(\bar{c}) = 30(\bar{c} - \bar{c}_0)^{0.22}$.

To perform the more accurate analysis and find the advantages of this or that tip part as for the value of sound pressure it is necessary to study tips of similar parameters.

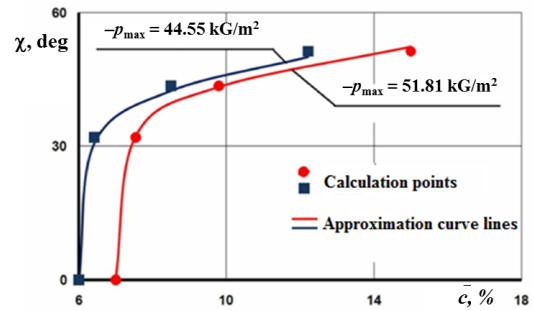


Figure 24 – Dependences of sweep angle and relative thickness of blade at the constancy of maximum sound pressure, taper $\eta=1$

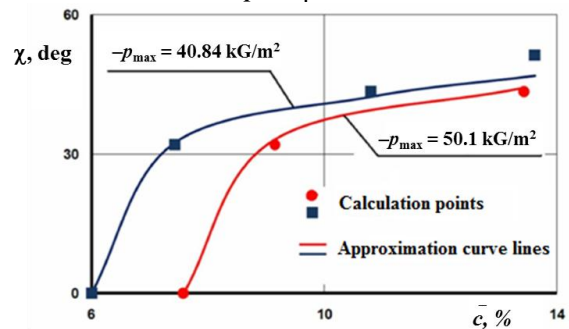


Figure 25 – Dependences of sweep angle and relative thickness of blade at the constancy of maximum sound pressure, taper $\eta=2$

Using the developed method and the calculation programme the numerical studies were performed for complex tips having different thicknesses and plane-forms to create the advanced high-speed helicopter. The calculation studies were made only for emitted sound pressure generated by the thickness of evaluated blades. The following parameters were taken for calculations: rotor radius – $R=7.315$ m, blade chord – $b=0.533$ m, blade profile – $NACA0012$, tip speed – $\omega R=250$ m/s, flight velocity $V_x=80$ m/s and constant relative thickness of blade $\bar{c}=12$ %. The relative thickness constancy is explained by the fact that the highest value of sound pressure generated by blade thickness is observed on the tip S since its absolute value in the neighbourhood of chord maximum value has increased. As the calculations show if

the blade tip S is varied as for its plane-form and thickness it is possible to sufficiently reduce the sound emission. Figure 26 shows the histogram of sound pressure maximum values $-p_{max}$ at constant relative thickness $\bar{c} = const$; the advantage of one tip over another is obvious here. Figure 27 shows the histogram of maximum sound pressure at constant absolute $c = const$.

When we have such data obtained for different tips we can sufficiently reduce the time to choose the rational blade parameters at the initial design stage.

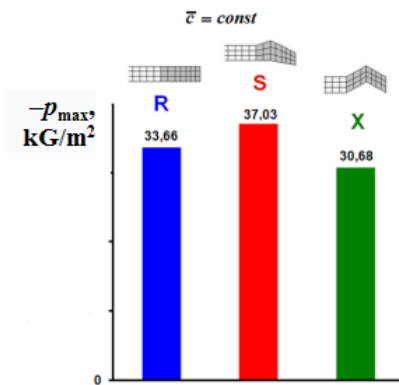


Figure 26 – Histogram of maximum sound pressure at constant relative thickness

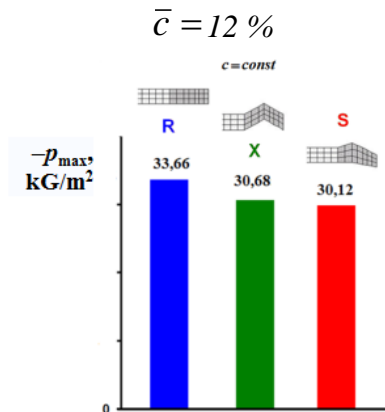


Figure 27 – Histogram of maximum sound pressure at constant absolute thickness

5. STUDIES OF SOUND PRESSURE RADIATION PATTERN

Figures 28 and 29 show the calculation and test radiation patterns of sound pressure in horizontal and vertical planes. Figure 28 shows the distribution of sound pressure in horizontal plane; Figure 29 – in vertical one at the distance equal to three rotor radii to the hub.

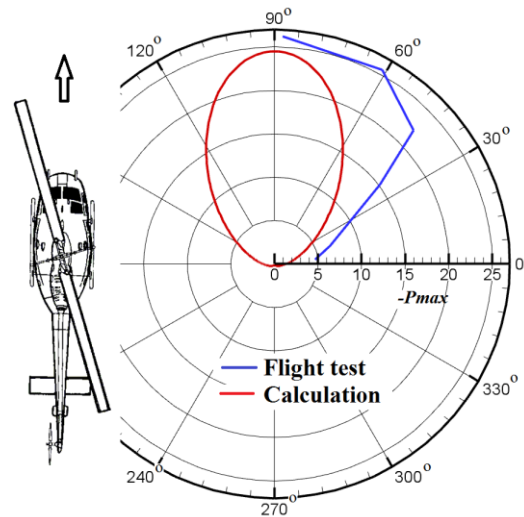


Figure 28 – Horizontal plane of radiation pattern

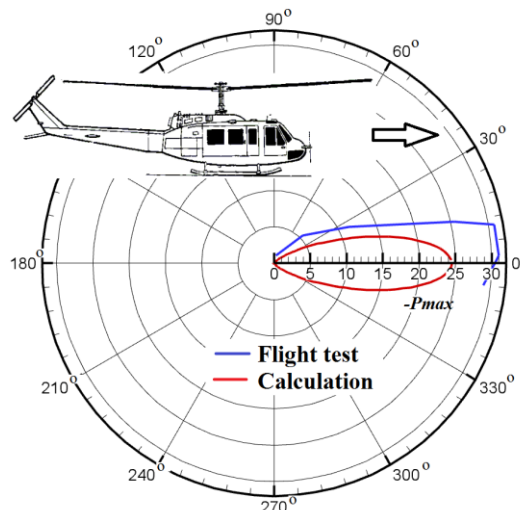


Figure 29 – Vertical plane of radiation pattern

Figures 30, 31 and 32 show the fields of sound pressure distribution obtained by calculations. Figure 30 shows a horizontal plane; Figure 31 shows a vertical plane and Figure 32 shows the plane behind the

helicopter at the distance of three radii. The clear cone of radiation in each plane is observed.

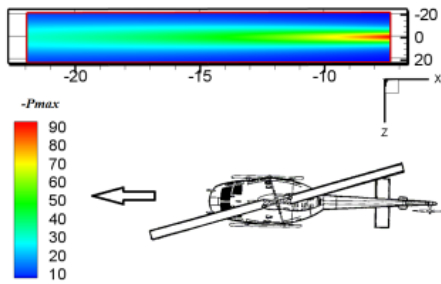


Figure 30 – Distribution of sound pressure in horizontal plane

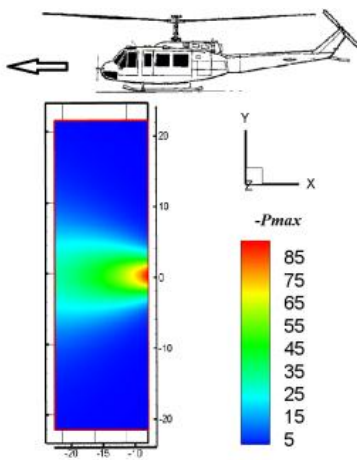


Figure 31 – Distribution of sound pressure in vertical plane

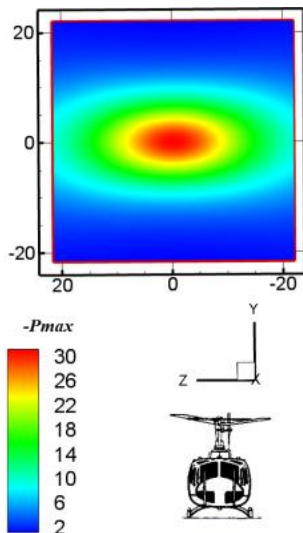


Figure 32 – Distribution of sound pressure in the plane normal to movement direction behind the helicopter

REFERENCES:

- 1 Aeroacoustics research – an army perspective h. Andrew Morse, Fredric H. Schmitz NASA Conference Publication 2052 Part I, Part II Helicopter Acoustics May 22-24, 1978.
- 2 Wayne Johnson Helicopter Theory. Princeton University Press 1980.
- 3 A. G. Munin, V. F. Samokhin et al. Aeronautical Acoustics. Edited by A. G. Munin – M., Mashinostroenie, 1986. In Russian.
- 4 V. E. Baskin Acoustic pressure generated by helicopter rotor in forward flight. TsAGI Proceedings, issue 1373, 1972. In Russian.
- 5 V. E. Baskin On linear theory of non-stationary gas motion under the action of non-potential external forces. Proceedings of the Russian Academy of Sciences. Mechanics of fluids No4, 1969. In Russian.
- 6 V. A. Golovkin, B. S. Kritsky, R. M. Mirgazov “On the calculations of main rotor thickness noise generated by blade thickness”, TsAGI Science Journal, v. XLI, No 5, 2010. In Russian.
- 7 Schmitz F.H., Boxwell D.A. “In-Flight Far-field Measurement of Helicopter Impulsive Noise”, 32nd Annual National Forum AHS Preprint № 1062, 1976.

Copyright Statement

The authors confirm that they, and/or their company or organization, hold copyright on all of the original material included in this paper. The authors also confirm that they are authorized, by the copyright holder of any third party material included in this paper, to publish it as a part of their paper. The authors confirm that they grant permission, or are authorized by the copyright holder of this paper, to

publish and distribute this paper as a part of ERF2013 proceedings or as individual offprints from the proceedings and for inclusion in a free access web-based repository.